The Astrophysical Journal, 662:738–743, 2007 June 10

PURE AMPLITUDE MASKS FOR EXOPLANET DETECTION WITH THE OPTICAL DIFFERENTIATION CORONAGRAPH

José E. Oti, Vidal F. Canales, and Manuel P. Cagigal
Departamento de Física Aplicada, Universidad de Cantabria, Avda. Los Castros S/N, E-39005, Santander, Cantabria, Spain;
jose.oti@gmail.com, fernancv@unican.es, perezcm@unican.es
Received 2006 May 31; accepted 2007 March 5

ABSTRACT

The optical differentiation coronagraph relies on the optical differentiation technique implemented on a standard coronagraph. The use of a coronagraphic mask to estimate the first derivative of the incoming field shows high starlight suppression (theoretically infinite), but it is highly sensitive to pointing errors and suffers from monochromaticity drawbacks. In order to overcome these limitations, we generalize the optical differentiation concept to higher order derivatives. Here we describe a novel set of coronagraphic masks that estimate the second derivative of the incoming field. A mathematical description of the optical differentiation coronagraph is presented. These new masks also achieve a theoretical perfect suppression of the on-axis light, and furthermore, they are less sensitive to pointing errors (fourth-order sensitivity to tip/tilt error leakage). Moreover, they are pure amplitude masks, and hence they do not require a complementary phase mask, which represents an additional advantage. The use of a Gaussian roll-off helps to concentrate the diffracted starlight near the pupil borders, where it could be removed more efficiently by a Lyot stop, and transforms the coronagraph into a nearly band-limited coronagraph.

Subject headings: astrobiology — instrumentation: high angular resolution — planetary systems — techniques: high angular resolution

1. INTRODUCTION

More than 150 exoplanets have already been detected by indirect methods. Despite this indirect detection success, direct detection of exoplanets is a topic of the greatest scientific interest, since it will allow their characterization through spectroscopy. Although great efforts have been made to obtain direct images of exoplanets, it remains a very difficult task. The large contrast ratio (10^9–10^{10} to 1 for an Earth-like exoplanet in the visible range) and the small angular separation between parent star and exoplanet makes its detection very difficult. In the last few years, several new coronagraphic concepts have been proposed to deal with these challenging requirements. The goal of these designs is to reveal the exoplanet by reducing the amount of starlight at its position. The latest coronagraphic designs achieve the required starlight suppression in the ideal case. Some of them use a modified coronagraphic mask implemented in a standard Lyot coronagraph (Lyot 1939). For instance, the four-quadrant phase-mask coronagraph uses a phase mask (Rouan et al. 2000), and the band-limited coronagraph proposed by Kuchner & Traub (2002) uses a specially designed amplitude mask.

Recently, the use of the optical differentiation technique as a coronagraphic procedure has been proposed by Oti et al. (2005b) in the optical differentiation coronagraph (ODC). The idea is to estimate the first derivative of the incoming field by the use of a differentiation mask instead of the standard occulting disk in a Lyot coronagraph. Since the parent star is on axis, its wave front is planar, and hence its derivative is equal to zero. On the other hand, the exoplanet is off axis so its wave front is tilted, and consequently its derivative is not zero. This coronagraphic concept achieves the required starlight suppression (theoretically it achieves total suppression), and it presents some interesting features, such as a small inner working angle. However, it presents some drawbacks, such as its high sensitivity to pointing errors, the requirement of rotating the mask to uncover all the possible exoplanets, or the use of a phase step to correctly construct the actual differentiation mask, implying an additional difficulty in its fabrication.

Following the optical differentiation concept, we extend it to estimate higher order derivatives with a new set of coronagraphic differentiation masks. These new masks overcome some of the limitations of the previous designs. In this work, we describe the second derivative coronagraphic masks, with quadratic amplitude transmittance, that theoretically allow total suppression of the on-axis light. These coronagraphic masks present the advantage of being polychromatic, since they are pure amplitude masks, and less sensitive to pointing errors than the first derivative masks. In addition, we present a novel design that avoids the requirement of rotating the coronagraphic masks. Furthermore, we use a Gaussian profile multiplying the mask, which allows an improvement on starlight extinction. Actually, the effect of the Gaussian profile is to transform the optical differentiation coronagraphic mask into a nearly band-limited mask. We have developed a mathematical description, based on the Fourier transform, that uses the derivative function to demonstrate how this approach works. Furthermore, this description is valid for all optical differentiation coronagraphs, and it is useful for evaluating the performance of different types of coronagraphic masks and window functions.

In § 2 the coronagraphic concept based on the optical differentiation technique is briefly described, and the second derivative coronagraphic masks are presented. We then analyze the effect of multiplying the differentiation mask by a Gaussian profile and its sensitivity to low-order aberrations. A mathematical description of the optical differentiation coronagraph, based on the Fourier transform, is presented. Next, the performance of these new masks is analyzed in § 3 from different points of view: mask coronagraphic extinction, sensitivity to pointing errors, and mask throughput. Finally, in § 4 some conclusions are presented.

2. THE OPTICAL DIFFERENTIATION CORONAGRAPH: THEORY AND MASK DESIGNS

2.1. *Optical Differentiation Technique*

The main idea underlying this coronagraphic concept is the use of the optical differentiation technique to suppress the on-axis

starlight. This method has been described thoroughly in previous works (Oti et al. 2003, 2005a). Hence, in this paper only a brief description of the optical differentiation technique is presented. The standard optical differentiation set-up consists of a telescopic system. The first lens performs the Fourier transform of the incoming field. Then, a mask whose amplitude transmittance linearly increases along one direction is placed at the intermediate focal plane, and finally, the second lens performs another Fourier transform. The output of this system is related to the first derivative of the incoming field, which is estimated along the mask slope direction. An unresolved star on the optical axis presents a plane wave front, and consequently its field derivative is equal to zero. On the other hand, an exoplanet is off axis and presents a tilted wave front, so its derivative is not zero. Furthermore, its detected intensity is directly related to the exoplanet's angular separation. The differentiation mask required to estimate the first derivative is described as $2\pi u_x i$, where u_x is the spatial frequency coordinate corresponding to the x-direction, and i is the imaginary unit. This mask is made of two different components: the first is a pure transmittance mask with amplitude transmittance proportional to $|2\pi x|$. The second is a $\pi/2$ phase step for the positive-valued coordinates and a $-\pi/2$ phase step for the negatives ones. This is required to attain the correct mask sign and also the imaginary unit (Iizuka 1987). Consequently, the first derivative is performed along the mask slope direction. The results obtained by the ODC look quite promising, since it is able to achieve deep starlight suppression and presents high performance in the detection of exoplanets under ideal conditions (Oti et al. 2005b). But it also presents some disadvantages, pointed out before.

2.2. *The Second Derivative Mask*

Following the same basic idea, and to overcome some of the limitations of the first derivative coronagraphic masks, we introduce the second derivative coronagraphic masks. From the definition of the Fourier transform, the second derivative of a function $f(x,y)$ along the x-direction can be expressed as

$$\frac{\partial^2 f(x,y)}{\partial x^2} = \int_{-\infty}^{\infty} (2\pi u_x i)^2 F(u_x,u_y) e^{2\pi i(xu_x+yu_y)}\, du_x\, du_y, \quad (1)$$

where $F(u_x,u_y)$ stands for the Fourier transform of the function $f(x,y)$, and u_x and u_y are the spatial frequency coordinates corresponding to the x- and y-direction. Therefore, using a mask of the form $(2\pi u_x)^2$, instead of the linearly increasing amplitude-transmittance mask, an optical differentiation set-up estimates the second derivative of the incoming field. The derivative is estimated along the direction in which the mask amplitude varies. Considering an electric field described as $E(x,y) = E_0 \exp(i\phi(x,y))$ at the entrance pupil of the coronagraph, where $\phi(x,y)$ is the wave front phase and E_0 is the constant amplitude of the field, the intensity detected at the coronagraphic pupil, $I(x,y)$, can be expressed as

$$I(x,y) = \left|\frac{\partial^2 E(x,y)}{\partial x^2}\right|^2 = |E_0|^2 \left[\left|\frac{\partial \phi(x,y)}{\partial x}\right|^4 + \left|\frac{\partial^2 \phi(x,y)}{\partial x^2}\right|^2\right]. \quad (2)$$

From this equation, it follows that the on-axis starlight is completely removed, since it presents a plane wave front phase, and therefore its derivative is equal to zero. Since the second derivative mask is a pure amplitude mask, it does not require the use of an additional phase mask, making its manufacture easier and avoiding monochromaticity drawbacks, which represents a great advantage with regard to the previous ODC coronagraphic mask designs.

2.3. *The Second Derivative Rotationally Symmetric Mask*

The mask described above estimates the second derivative along one direction. Since planets along the directions perpendicular to the mask amplitude variation give null derivatives, they do not become visible in the final image. Therefore, a rotation of the mask is required to perform a complete survey on all possible exoplanet locations. To avoid this rotation, we propose the use of a rotationally symmetric second derivative mask with an amplitude transmittance profile, described as $(2\pi)^2(u_x^2 + u_y^2)$. Hence, the intensity detected with this second derivative symmetric mask at the coronagraphic pupil can be expressed as

$$\begin{aligned} I(x,y) &= \left|\frac{\partial^2 E(x,y)}{\partial x^2} + \frac{\partial^2 E(x,y)}{\partial y^2}\right|^2 \\ &= |E_0|^2 \left[\frac{\partial^2 \phi(x,y)}{\partial x^2} + \frac{\partial^2 \phi(x,y)}{\partial y^2}\right]^2 \\ &\quad + |E_0|^2 \left\{\left[\frac{\partial \phi(x,y)}{\partial x}\right]^2 + \left[\frac{\partial \phi(x,y)}{\partial y}\right]^2\right\}^2. \end{aligned} \quad (3)$$

In this case, the mask estimates the second derivative along the x- and y-direction simultaneously. As a consequence, it is no longer necessary to rotate the mask to search for all the possible exoplanets around the parent star. This implies a gain in the coronagraph efficiency, allowing a more rational use of the available observing time. Theoretically, the masks described in this work achieve a perfect cancellation of the on-axis light source for a perfect wave front.

Finally, it is interesting to note that masks performing derivatives of an even order achieve an on-axis starlight extinction level comparable to that of the second derivative mask. What is more, the coronagraph performance (throughput, pointing error sensitivity, etc.) can be controlled using an appropriate combination of even-order differentiation masks, described as a power series expansion of even-order terms, keeping a high extinction level.

2.4. *The Gaussian Profile Roll-Off*

Since an actual finite second derivative mask ends sharply, the edge-diffracted starlight leaks into the coronagraph, raising the background light level. To avoid this background, we multiply the differentiation mask by a Gaussian profile so that it ends smoothly. As second derivative masks are pure amplitude masks, it is necessary to normalize them so that the transmittance ranges from zero to one. The final coronagraphic mask profile is plotted in Figure 1. The shape of these masks is mainly determined by the width of the Gaussian profile.

To explore the effect of the Gaussian profile, let us consider a simplified one-dimensional model of the ODC, shown in Figure 2. We follow a description similar to that given by Sivaramakrishnan et al. (2001). In the absence of atmospheric turbulence or phase errors, an on-axis source produces an electric field with constant amplitude and phase in an unobstructed telescope. We study the electric field as it goes through the coronagraph depicted in Figure 2. We focus our study on three planes, labeled a, b, and c, that correspond to the aperture pupil plane of the ODC, the image plane of the first lens, and the Lyot stop plane. The electric fields in these planes are related by the Fourier transform.

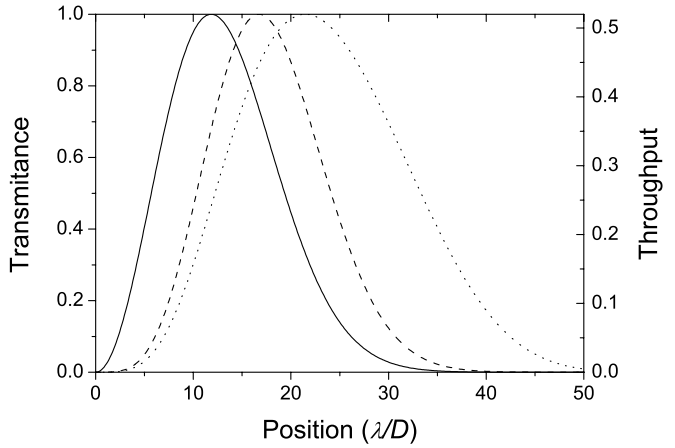

FIG. 1.—Amplitude transmittance of the coronagraphic masks and throughput of the optical differentiation coronagraph. Cross section along the x-direction for the first derivative (*solid curve*) and second derivative (*dashed curve*) coronagraphic masks. The dotted curve corresponds to a second derivative coronagraphic mask with three nonzero mean Gaussian profiles.

First, the incoming electric field passes through the aperture pupil of the coronagraph (Fig. 2*a*), described by a stop function, $\Pi(x/D)$, which is equal to 1 inside the pupil of size D and zero outside. The electric field at the image plane is the Fourier transform of the electric field at the aperture pupil. It is described by the sinc (uD) function (Fig. 2*b*), where u is the spatial frequency coordinate corresponding to the x-coordinate. In the ODC, the image plane electric field is modified by a differentiation mask. Here we study the particular case of a second derivative differentiation mask whose amplitude transmittance varies quadratically with position, $M(u) \propto u^2$. Furthermore, the coronagraphic mask we propose is the product of this differentiation mask times a Gaussian profile $G(u) = \exp(-u^2/\omega)$. The width of the Gaussian profile (ω) is taken so that the final coronagraphic mask covers a large area of the image plane. Therefore, at the image plane, we have the product of the aperture pupil Fourier transform times the quadratic amplitude transmittance mask times the Gaussian profile. The final electric field at the Lyot stop plane, $E_{\rm LS}$, is proportional to the Fourier transform of this product:

$$E_{\rm LS}(x) \propto \mathrm{FT}[\mathrm{sinc}\,(uD)M(u)G(u)] = \mathrm{FT}[u\mathrm{FT}(\Pi(x/D))] * \mathrm{FT}[u\mathrm{FT}(g(x))], \quad (4)$$

where $*$ denotes convolution. Consequently, by recalling the differentiation property of the Fourier transform, we have that the electric field at the Lyot stop plane (Fig. 2*c*) is the first derivative of the stop function, $\Pi(x/D)$, convolved with the first derivative of the narrow Gaussian profile $g(x) = \mathrm{FT}(G(u))$. The first derivative of the stop function is equal to zero both inside and outside the aperture pupil, and it is only different from zero at the pupil borders, where a discontinuity occurs. Indeed, at the pupil borders, the value of the derivative is equal to infinity. The derivatives in these discontinuities can be described by two Dirac delta functions, $\delta(x + D/2)$ and $-\delta(x - D/2)$, located at the pupil borders. The first derivative of the Gaussian profile is $g'(x) \propto g(x)x$, where $g(x) \propto \exp(-x^2\omega)$ is a narrow Gaussian function of width $1/\omega$. The convolution gives a copy of the $g'(x)$ function at the positions corresponding to the Dirac delta function (Fig. 2*c*). Consequently, the light of the on-axis source is gathered near the pupil borders in a region controlled by the Gaussian width. This area is small, since, by mask design, ω is large. On the other hand, the central region of the Lyot stop plane presents a light level that is nearly zero, since the narrow Gaussian profile falls to negligible values near the pupil borders. Now, by applying a Lyot stop small enough to remove this light in the proximities of the pupil border, a good level of starlight suppression is achieved without a great disturbance of the exoplanet light.

Although this is a simplified model of the coronagraph, this mathematical development is useful for easily evaluating the coronagraphic performance of any kind of window functions. It provides an estimate of the capabilities of the different coronagraphic masks. Moreover, this description can be applied to all optical differentiation coronagraph proposals.

Our proposal of using a differentiation mask multiplied by a Gaussian profile is not a band-limited mask in the strict sense, but in practice both have a similar behavior. Indeed, the area in which our coronagraphic mask gathers the on-axis light is smaller than that of a band-limited mask coronagraph. The Lyot stop size required to achieve a very good level of starlight extinction with the ODC is about 80% of the entrance pupil, which is large compared to the Lyot stop required in the band-limited case, which is about 60% of the entrance pupil (Kuchner et al. 2005). Moreover, a further reduction of the ODC Lyot stop does not produce an appreciable improvement on starlight extinction, since all the energy is tightly located near the pupil borders. In consequence, the coronagraph's throughput is maximized, and the amount of light available to form the exoplanet image increases, thus improving its detection efficiency.

2.5. *Low-Order Aberration Sensitivity*

We perform a simple low-order aberration sensitivity analysis for the ODC coronagraphic mask. We follow the procedure described by Shaklan & Green (2005). Let us consider a complex field at a pupil of radius r, described with a pupil amplitude function $P(x)$ and a phase function $\phi(x) \ll 1$. This field can be expanded into a series as

$$E(x) = P(x)e^{i\phi(x)} = P(x)\left[1 + \sum_{l=1,2,3,\ldots} \frac{i^l}{l!}\phi^l(x)\right], \quad (5)$$

where the pupil amplitude function $P(x)$ is equal to 1 inside the aperture pupil and zero outside. At the focal plane of the first lens, we have the Fourier transform of the incoming field, $\hat{E}(u) = \mathrm{FT}(E(x))$. Then, the second-derivative coronagraphic mask is used and another Fourier transform is performed. The final field under this approximation is described as

$$F(x) = \mathrm{FT}\big(\hat{E}(u)\hat{M}(u)\big) = \frac{\partial^2}{\partial x^2}\left\{P(x)\left[1 + \sum_{l=1,2,3,\ldots} \frac{i^l}{l!}\phi^l(x)\right]\right\}. \quad (6)$$

This equation vanishes for any phase aberration whose x-coordinate dependence is less than second order. To see a tip/tilt leakage [i.e., $\phi(x) = 2a_2x + 2a_3y$], we require the second term of the wave expansion, $\phi(x)^2$. Thus, the intensity is expressed as

$$I(x) = |F(x)|^2 \propto a_2^4/(2!)^2. \quad (7)$$

Equation (7) shows that the ODC presents fourth-order behavior for the tip/tilt leakage. Furthermore, this low-order aberration sensitivity analysis is valid for the entire image plane, since no approximations have been made in the mathematical description of the second derivative mask $\hat{M}(u)$. This fourth-order dependence on tip/tilt error represents the minimum requirement for a

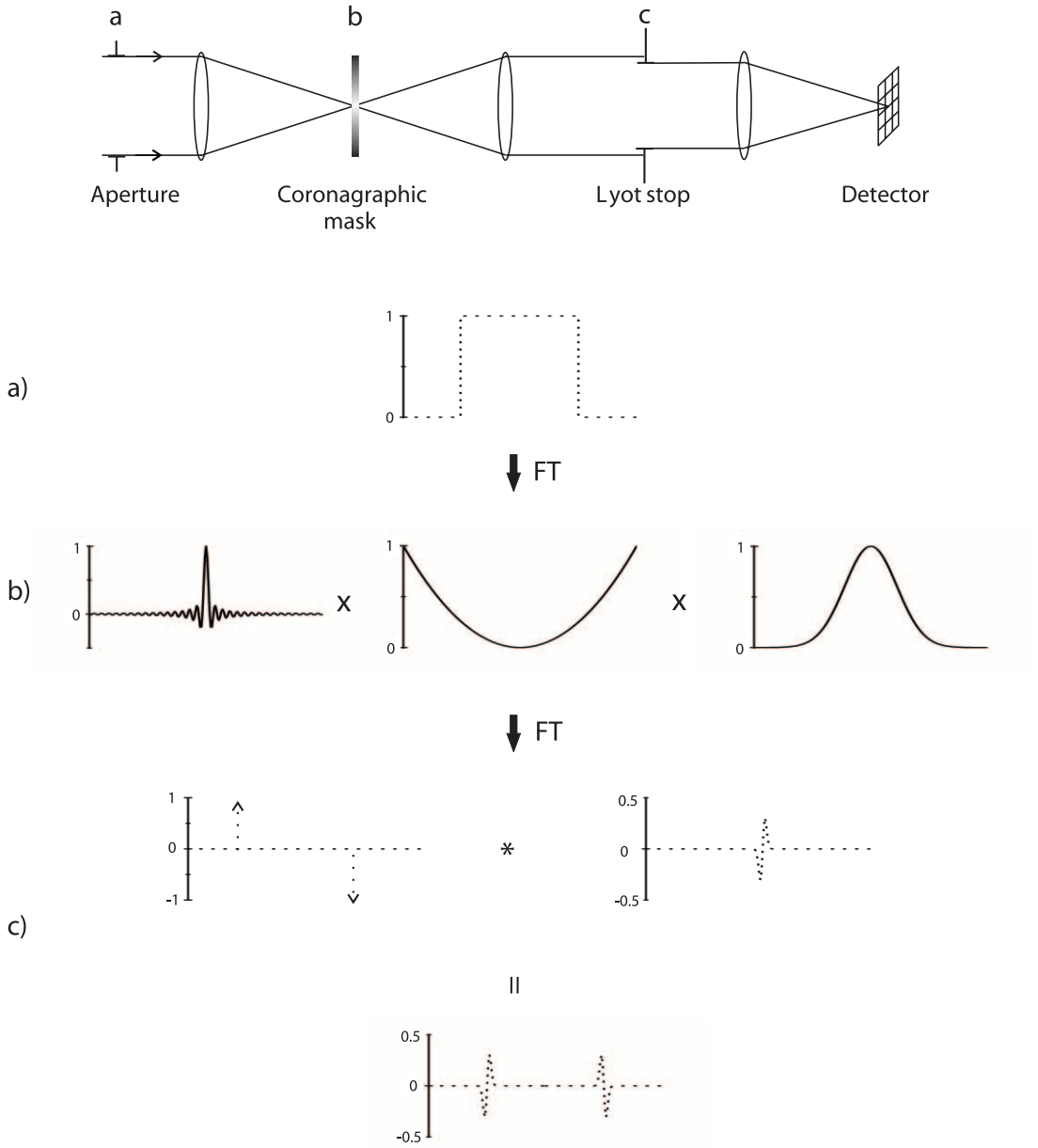

FIG. 2.—Set-up of the optical differentiation coronagraph and one-dimensional plots of the (*a*) aperture pupil of the coronagraph, $\Pi(x/D)$, (*b*) the electric field after the mask, which is the product of the function sinc (uD) times the second derivative coronagraphic mask $M(u)$ and the Gaussian profile $G(u)$, and (*c*) the resulting electric field at the Lyot stop plane, which is the convolution of the aperture pupil derivative with the derivative of the Gaussian function $g(x)$.

coronagraph to be taken into account for the *Terrestrial Planet Finder-Coronagraph* (*TPF-C*) mission (Quirrenbach 2005).

3. ODC CORONAGRAPHIC MASK PERFORMANCE

To check the coronagraphic performance of this new set of differentiation masks and to compare it with the first derivative mask, we have carried out computer simulations of the ODC under ideal conditions. The ODC has been simulated using the fast Fourier transform routine (Press et al. 1995). To achieve a good sampling and to avoid aliasing effects, we use large arrays of 1024×1024 data samples. The coronagraph pupil is simulated with a data sampling of 128×128. The Lyot stop is set to 85% of the aperture pupil of the coronagraph in all cases. The coronagraphic masks, represented in Figure 1, are simulated with a finite size of about $90\lambda/D$. Figure 1 shows a cross section along the x-direction of the amplitude transmittance of the first derivative mask (*solid curve*) and the second derivative mask (*dashed curve*). We represent the mask values corresponding to the positive x-coordinate, since it is an even mask. The second derivative symmetric mask is equal to the second derivative mask cross section in all directions, since it is a rotationally symmetric mask. The first derivative mask requires the use of a phase step to achieve the correct sign and the imaginary unit i.

3.1. *Starlight Suppression*

First, we check the level of starlight suppression achieved by the different kinds of differentiation masks on the ODC. We carry out the simulations under ideal conditions, with no phase distortion on the original wave front or pointing errors. The results of these simulations are shown in Figure 3. Profiles of the detected intensity simulated for the first derivative differentiation mask (*solid curve*), the second derivative (*dashed curve*), and the symmetric second derivative mask (*dotted curve*) are shown. It can be seen that all the coronagraphic masks achieve deep enough starlight extinction. The optimal Lyot stop size for the second derivative coronagraphic mask is about 80% of the entrance pupil, but

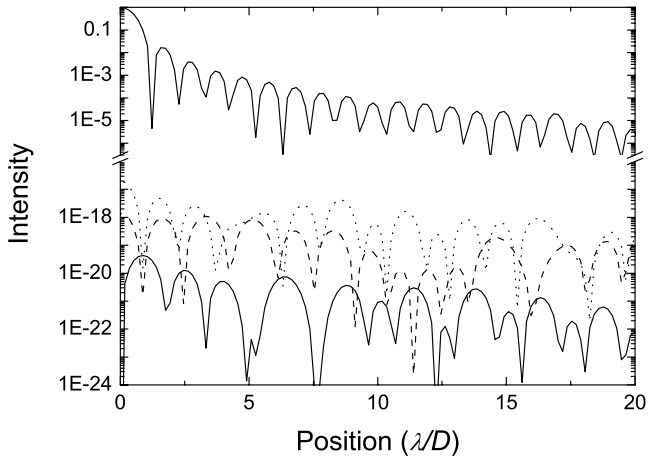

FIG. 3.—Simulated radial intensity profiles at 45° from the *x*-axis, obtained with the optical differentiation coronagraph using the first derivative (*solid curve*), second derivative (*dashed curve*), and the symmetric second derivative (*dotted curve*) coronagraphic masks. The masks used in these simulations are plotted in Fig. 1, the Lyot stop is set to 85% of the entrance pupil of the coronagraph, and the simulations are carried out for the ideal case (no wave front or pointing errors). The upper curve is the intensity profile without coronagraph and is plotted for comparison.

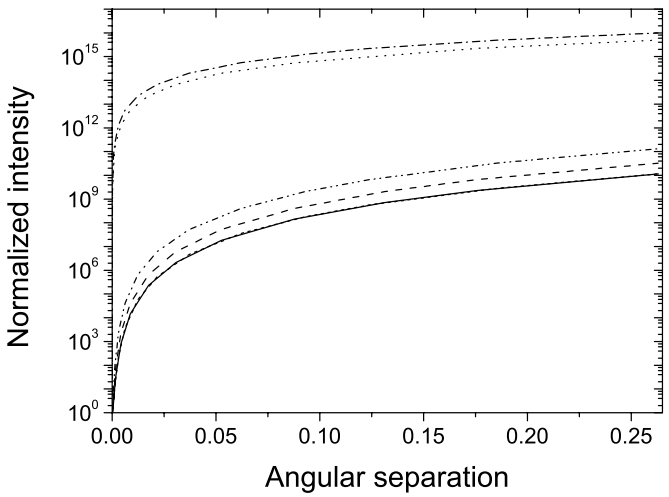

FIG. 4.—Normalized intensity obtained with the optical differentiation coronagraph as a function of the star displacement. The intensity is normalized to the extinction level achieved without pointing errors. The curves show the performance of the coronagraph when a star displacement along the *x*-axis is made, when the first derivative (*dash-dotted curve*), second derivative (*double-dot–dashed curve*), and symmetric second derivative (*solid curve*) coronagraphic masks are used. For a diagonal star displacement, the dotted curve corresponds to the first derivative mask and the dashed curve corresponds to the second derivative mask. The symmetric second derivative curve lies over the one corresponding to the *x*-axis case (*solid curve*).

in order to compare all the masks under similar conditions, we have used a Lyot stop size of 85% of the pupil, which is optimal for the first derivative mask. As a consequence, the first derivative mask performs slightly better than the other masks. However, even using this nonoptimal Lyot stop size, the achieved starlight extinction is large enough to allow exoplanet detection under ideal conditions.

3.2. *Sensitivity to Pointing Errors*

Following the same error estimation procedure described in § 2.5, it is easy to show that the first derivative mask presents a second-order sensitivity to tip/tilt error. The second derivative mask should be less affected by pointing errors, since it presents a fourth-order sensitivity to tip/tilt errors. To check it, we have performed computer simulations of the ODC with both first and second derivative coronagraphic masks. The results of these simulations are shown in Figure 4. The central star is slightly moved out of the optical axis, both along the *x*-axis (derivative direction) and along the diagonal direction (45°). The intensity measured is normalized to the intensity measured with no pointing error and is plotted as a function of the star angular separation from the optical axis. Hence, this figure shows the degradation in coronagraphic performance as a consequence of the pointing errors. The first derivative coronagraphic mask presents an almost immediate response to the pointing error, and the starlight leakage is large for the *x*-direction (*dash-dotted curve*) and the diagonal direction (*dotted curve*) pointing errors. The second derivative coronagraphic mask presents a slower increase in the starlight leakage for both the *x*-direction (*double-dot–dashed curve*) and the diagonal direction (*dashed curve*) pointing errors. In the previous cases, the 45° pointing error is smaller, since the trace of the star over the darker part of the differentiation masks is larger than in the *x*-direction case. The second derivative symmetric mask has even better performance than the other differentiation masks (*solid curve*), and as expected, its response is the same for pointing errors along any direction.

3.3. *Mask Throughput*

Another important parameter to evaluate the coronagraphic performance in exoplanet detection is the coronagraphic mask throughput. Figure 1 shows the throughput for the two derivative coronagraphic masks analyzed here. The first derivative mask (*solid curve*) presents better throughput in the proximity of the parent star than the second derivative masks (*dashed curve*). Although this implies a greater sensitivity to pointing errors, as we have shown in the previous section.

It is also possible to increase the coronagraphic mask throughput in the outer region, called the outer working angle, by multiplying the second derivative mask by a function composed by the addition of several Gaussian profiles. These Gaussian profiles are centered at different positions and have different widths. The effect of using this mask can be seen in the example shown in Figure 1 (*dotted curve*). With this approach, it is possible to increase the outer working angle without a significant decrease in the coronagraph performance.

Another method of increasing the coronagraph throughput is to obtain a mask function as a proper combination of even-order polynomials (i.e., the truncated expansion of the function 1 − Gaussian). Thanks to the linearity of the Fourier transform, the final field can be described as a series of even derivatives weighted by the coefficients of the series expansion.

Moreover, it is necessary to multiply by a Gaussian profile to reduce the mask value to zero for large *x*-values. Hence the starlight extinction is theoretically infinite. If the series expansion starts in the second-order term, the final tip/tilt leakage is going to be of fourth order. This could be improved by starting the series with the fourth-order term; then the final tip/tilt leakage will be of eighth order.

4. CONCLUSIONS

Here we present a novel set of coronagraphic masks to be used in a standard Lyot coronagraph. These new masks perform the second derivative of the incoming field. To estimate the second derivative, a mask whose amplitude transmittance varies quadratically along the derivative direction is needed. As a consequence, this mask is a pure amplitude mask, and it therefore avoids the chromatic limitations that arise from the use of the phase step required

for the first derivative coronagraphic mask. This represents a great advantage, and makes its manufacture easier. Furthermore, a symmetric second derivative mask is described. This mask estimates the second derivative along the x- and y-directions simultaneously, so the rotation of the mask is no longer required to make a complete survey of the possible exoplanets, representing a further advantage. These second derivative masks present fourth-order behavior for the tip/tilt leakage, and hence they are less sensitive to pointing errors. In addition, these masks are multiplied by a Gaussian profile that allows an improvement of its coronagraphic performance. The actual effect of the Gaussian profile is to transform the optical differentiation coronagraph into a nearly band-limited coronagraph. Finally, simulations to check the performance of the optical differentiation coronagraph carried out under ideal conditions show that the level of starlight extinction achieved is deep enough to allow exoplanet detection and that throughput and sensitivity to pointing error can be controlled from the mask design.

This work was supported by Ministerio de Ciencia y Tecnología AYA2004-07773-C02-01. J. E. Oti was supported by a FPU grant of the Ministerio de Educación y Ciencia.

REFERENCES

Iizuka, K. 1987, Engineering Optics (Berlin: Springer)
Kuchner, M. J., Crepp, J., & Ge, J. 2005, ApJ, 628, 466
Kuchner, M. J., & Traub, W. A. 2002, ApJ, 570, 900
Lyot, B. 1939, MNRAS, 99, 580
Oti, J. E., Canales, V. F., & Cagigal, M. P. 2003, Opt. Express, 11, 2783
———. 2005a, MNRAS, 360, 1448
———. 2005b, ApJ, 630, 631
Press, W. H., Teuklosky, S. A., Vetterling, W. T., & Flannery, B. P. 1995, Numerical Recipes in C (2nd ed.; Cambridge: Cambridge Univ. Press)
Quirrenbach, A. 2005, preprint (astro-ph/0502254)
Rouan, D., et al. 2000, PASP, 112, 1479
Shaklan, S. B., & Green, J. J. 2005, ApJ, 628, 474
Sivaramakrishnan, A., et al. 2001, ApJ, 552, 397